The Journal of Immunology

Citrullination Controls Dendritic Cell Transdifferentiation into Osteoclasts

Akilan Krishnamurthy, A. Jimmy Ytterberg, Meng Sun, Koji Sakuraba, Johanna Steen, Vijay Joshua, Nataliya K. Tarasova, Vivianne Malmström, Heidi Wähämaa, Bence Réthi and Anca I. Catrina

J Immunol 2019; 202:3143-3150; Prepublished online 24 April 2019;
doi: 10.4049/jimmunol.1800534
http://www.jimmunol.org/content/202/11/3143

The Journal of Immunology is published twice each month by
The American Association of Immunologists, Inc.,
1451 Rockville Pike, Suite 650, Rockville, MD 20852

Print ISSN: 0022-1767 Online ISSN: 1550-6606.

Citrullination Controls Dendritic Cell Transdifferentiation into Osteoclasts

Akilan Krishnamurthy,* A. Jimmy Ytterberg,*,† Meng Sun,* Koji Sakuraba,*,‡ Johanna Steen,* Vijay Joshua,* Nataliya K. Tarasova,† Vivianne Malmström,* Heidi Wähämaa,* Bence Réthi,* and Anca I. Catrina*

An increased repertoire of potential osteoclast (OC) precursors could accelerate the development of bone-erosive OCs and the consequent bone damage in rheumatoid arthritis (RA). Immature dendritic cells (DCs) can develop into OCs, however, the mechanisms underlying this differentiation switch are poorly understood. We investigated whether protein citrullination and RA-specific anti–citrullinated protein Abs (ACPAs) could regulate human blood–derived DC–OC transdifferentiation. We show that plasticity toward the OC lineage correlated with peptidyl arginine deiminase (PAD) activity and protein citrullination in DCs. Citrullinated actin and vimentin were present in DCs and DC-derived OCs, and both proteins were deposited on the cell surface, colocalizing with ACPAs binding to the cells. ACPAs enhanced OC differentiation from monocyte-derived or circulating CD1c$^+$ DCs by increasing the release of IL-8. Blocking IL-8 binding or the PAD enzymes completely abolished the stimulatory effect of ACPAs, whereas PAD inhibition reduced steady-state OC development, as well, suggesting an essential role for protein citrullination in DC–OC transdifferentiation. Protein citrullination and ACPA binding to immature DCs might thus promote differentiation plasticity toward the OC lineage, which can facilitate bone erosion in ACPA-positive RA. ***The Journal of Immunology*****, 2019, 202: 3143–3150.**

Activated dendritic cells (DCs) can migrate to lymphoid tissues to induce T cell activation, clonal expansion, and differentiation into specialized cellular subsets (1). In contrast, non- or suboptimally activated DCs promote Ag-specific tolerance, thereby suppressing autoimmune reactions under steady-state conditions (2, 3). DCs can thus initiate strikingly different immune responses because of a high level of functional plasticity, which is a result of their own developmental diversity and an adaptation to different types of activation signals and tissue-derived factors, such as cytokines, metabolites, or other immunoregulatory compounds (1, 4). Such plasticity can also allow DCs to transdifferentiate into other cell types, among them osteoclasts (OCs), in response to M-CSF and RANKL (5, 6). Interestingly, inflammatory mediators present in the synovial fluid of rheumatoid arthritis (RA) patients promote DC transdifferentitation into OCs (5). Cytokines, degradation products of the extracellular matrix or, alternatively, the glycolytic microenvironment, have been implicated in promoting DC–OC transition and thereby exacerbating bone damage (5, 6); however, the exact mechanisms that turn DCs into precursors for OC differentiation have not yet been clarified.

OCs can typically develop from monocytes and macrophages (MΦs) in the presence of RANKL and M-CSF, and we have recently demonstrated that this process is dependent on citrullination, a posttranslational modification catalyzed by peptidyl arginine deiminase (PAD) enzymes (7). Abs targeting citrullinated proteins (anti–citrullinated protein Abs [ACPAs]) are present in the peripheral blood (PB) of a majority of patients suffering from RA, and ACPA positivity is associated with increased bone loss in these patients (8). ACPAs purified from the synovial fluid and PB of RA patients were able to enhance MΦ-derived osteoclastogenesis in vitro and induce bone loss when injected in mice (7, 9).

We hypothesized that citrullination could play a role in DC transdifferentiation into OCs, and Abs against citrullinated proteins might represent previously unknown mediators that turn DCs into OC precursors in the inflammatory milieu of RA. To test this hypothesis, we first characterized PAD activities and protein citrullination during the development of OCs from DC precursors, and then we investigated the impact of ACPAs on this process.

Materials and Methods

Patients

SF and plasma samples (n = 26 and 38, respectively) were collected at the Rheumatology Clinic at Karolinska University Hospital from RA patients

*Rheumatology Unit, Karolinska University Hospital, Karolinska Institutet, S-171 76 Stockholm, Sweden; †Department of Medical Biochemistry and Biophysics, Karolinska Institutet, SE-171 77 Stockholm, Sweden; and ‡Clinical Research Institute, National Hospital Organisation, Kyushu Medical Center, Fukuoka 810-8563, Japan

ORCIDs: 0000-0002-9301-0421 (M.S.); 0000-0003-2171-614X (K.S.); 0000-0001-9251-8082 (V.M.).

Received for publication April 16, 2018. Accepted for publication March 21, 2019.

This work was supported by the FOREUM Foundation for Research in Rheumatology, the European Research Council under European Union Horizon 2020 Research and Innovation Program Grant Agreements CoG 2017 - 7722209_PREVENT RA and 777357_RTCure, the Swedish Research Council, and the King Gustaf V's and Queen Victoria's Foundation.

A.K. and A.I.C. designed the study and developed the concept together with A.J.Y., M.S., H.W., and B.R. A.K. wrote the manuscript together with A.I.C. and B.R. A.K. performed and analyzed all OC assays with help from K.S. A.J.Y. performed the mass spectrometry analysis with help from N.K.T. A.K. and V.J. measured the cytokines using cytometric bead array. M.S. and A.K. performed the immunofluorescence staining. H.W. purified the polyclonal ACPAs, and J.S. and V.M. produced the monoclonal ACPA. B.R. measured PAD activities. All authors critically reviewed and approved the final form of the manuscript.

Address correspondence and reprint requests to Dr. Akilan Krishnamurthy, Rheumatology Unit, Department of Medicine, Karolinska University Hospital and Karolinska Institutet, S-171 76 Stockholm, Sweden. E-mail address: akilan.krishnamurthy@ki.se

Abbreviations used in this article: ACPA, anti–citrullinated protein Ab; DC, dendritic cell; iDC, immature DC; MΦ, macrophage; OC, osteoclast; PAD, peptidyl arginine deiminase; PB, peripheral blood; PCA, principal component analysis; RA, rheumatoid arthritis; TRAP, tartrate-resistant acid phosphatase.

fulfilling the 1987 American College of Rheumatology classification criteria. All patients were characterized by high levels of anti-CCP2 Abs (at least three times higher than the cutoff levels, as determined using a CCP2 ELISA kit [Eurodiagnostica, Malmö, Sweden]). Informed consent was obtained from all patients in accordance with the protocol approved by the Ethical Review Committee North of Karolinska University Hospital. Total IgG was isolated on a Protein G column, whereas ACPAs were isolated on CCP2 columns as described previously (10). The flow-through fraction from CCP2 columns was used as IgG control. Fresh blood samples from ACPA-positive RA patients (n = 4, three females and one male; median age, 51) or buffy coats from healthy individuals were collected for monocyte and immature DC (iDC) isolation.

OC culture and bone resorption assay

Mononuclear cells were isolated from the PB by Ficoll centrifugation (GE Healthcare Bioscience, Uppsala, Sweden), which was followed by monocyte separation using anti-CD14–conjugated microbeads (Miltenyi Biotec Norden, Lund, Sweden). These cells were used to develop iDCs and MΦs. Briefly, dense and sparse cultures of $CD14^+$ monocytes were established using a final cellular density of 2×10^6 cells/ml or 0.125×10^6 cells/ml, respectively, and the cells were differentiated into iDCs in six-well plates using RPMI 1640 medium supplemented with 10% heat-inactivated FBS, 2 mM L-glutamine, 100 IU/ml penicillin, and 50 μg/ml streptomycin (all from Sigma-Aldrich, Stockholm, Sweden), as well as 75 ng/ml GM-CSF and 50 ng/ml IL-4 (both from PeproTech, London, U.K.) for 6 d (6). Equal numbers of either dense or sparse culture–derived iDCs were then seeded at a final density of 5×10^5 cells/ml in 96-well plates in DMEM containing 25 ng/ml M-CSF (PeproTech) and 50 ng/ml RANKL (R&D Systems, Abingdon, U.K.) and cultured for 12–14 d. In parallel, $CD14^+$ monocytes were cultured at a final cellular density of 1×10^6 cells/ml and differentiated into MΦs in six-well plates in DMEM supplemented with FBS, L-glutamine, penicillin, and streptomycin, as described above, in the presence of 25 ng/ml M-CSF for 3 d. MΦs were then cultured in 24-well plates in DMEM containing 10 ng/ml M-CSF and 5 ng/ml RANKL and cultured for 10–12 d. Blood $CD1c^+$ DCs were isolated using the CD1c $(BDCA\text{-}1)^+$ Dendritic Cell Isolation Kit (Miltenyi Biotec), and cell purity was checked by flow cytometry (median purity of 93%, range 86–99%). ACPAs and control IgG were added to the cultures when indicated. The ACPA and control IgG fractions did not contain LPS contamination, according to the limulous amebocyte lysate test. In addition, Ab preparations were negative when tested on the THP1-XBlue-MD2-CD14 reporter cell line (InvivoGen, San Diego, CA) and HEK-Blue hTLR2 reporter assay (InvivoGen).

$F(ab')_2$ ACPAs and control IgGs were generated using a commercially available kit (Genovis, Lund, Sweden) and used at equal molarity as the intact Abs. Cytokines, Abs, and 50% of the medium were replenished every third day. The cell cultures were stained with the leukocyte acid phosphatase kit from Sigma-Aldrich, and OCs were identified in light microscopy as tartrate-resistant acid phosphatase $(TRAP)^+$ cells with at least three nuclei. In parallel, OCs were developed in 96-well plates coated with synthetic calcium phosphate (Big Flats, Corning, NY). The cells were removed by chlorine bleach, and erosion areas were quantified using NIS Elements (Nikon Instruments Europe, Amsterdam, the Netherlands) by spotting two random fields per well under ×4 magnification. The IL-8 neutralizing Ab (clone: MAB208; R&D Systems) was used at a 1-μg/ml concentration, and Cl-amidine (Cayman Chemical, Ann Arbor, MI) to block PAD activation was used in a range of 0.2–200 μM.

Mass spectrometry

Proteins were extracted from cell pellets lysed in 8 M urea in 100 mM ammonium bicarbonate by sonication on ice. The protein concentrations were determined using the BCA method (BCA kit; Thermo Scientific, Bremen, Germany). Following reduction and alkylation, 10 μg of proteins was digested by trypsin at a ratio of 1:30 trypsin:protein in the presence of 1% ProteaseMAX (all reagents from Promega, Nacka, Sweden). Digestion was stopped with formic acid. Digests were cleaned with Stage Tips (Thermo Scientific), dried, and resuspended in 0.1% formic acid prior to analysis. Liquid chromatography-tandem mass spectrometry analyses were performed using an Easy-nLC chromatography system directly coupled online to a Q Exactive mass spectrometer (Thermo Scientific). The list of identified proteins was further filtered using 1% false discovery rate. The proteomes were compared by performing a principal component analysis (PCA) of the normalized, log-transformed protein areas using SIMCA 13.0.3 (Umetrics, Umeå, Sweden). Default settings were used, with the exception of using Par scaling. Model performance was reported as cumulative correlation coefficients for the model (R2X[cum]) and predictive performance based on 7-fold cross-validation calculations (Q2[cum]). By default, proteins with missing values in 50% of the comparisons were removed.

Peptide identification and validation

Mass lists were extracted and processed according to a previously described protocol (11) and searched against the SwissProt database (release 2013_04; 40,492 human sequences) using the Mascot search engine version 2.3.02 (Matrix Science, London, U.K.). The following parameters were used: trypsin digestion with a maximum of two missed cleavages; carbamidomethylation as a fixed modification; pyroglutamate, oxidation, and citrullination were used as variable modifications; a precursor mass tolerance of 10 ppm; and a fragment mass tolerance 0.1 Da. The list of identified proteins was further filtered by using 1% false (peptide level) and requiring at least two matching peptides for each protein. Quantification was performed using Quanti (11), a program for label-free quantification.

All peptides identified as citrullinated were carefully validated manually. Special attention was given to correct precursor mass assignment, retention time shifts (where appropriate), and correct shifts in fragment masses around the modified site. Only peptides for which the modified site could be unambiguously determined are reported.

Flow cytometry

Cells were labeled using FITC-conjugated anti-CD14 and PE-conjugated anti-CD1a Abs (BD Pharmingen, San Jose, CA) or with PE-conjugated anti-CXCR1, allophycocyanin-conjugated anti-CXCR2 (BioLegend, San Diego, CA), PerCP/Cy5.5-conjugated anti-BDCA1 (CD1c), or isotype control Abs from BioLegend. Samples were analyzed using a Gallios flow cytometer (Beckman Coulter) and the Flow Jo software version 9.2 (Ashland, OR).

Cytokine analysis

Cytokine levels were analyzed using the Cytometric Bead Array (BD Biosciences, San Diego, CA) according to the manufacturer's instructions.

PAD activity assay

Briefly, cell pellets were lysed using radioimmunoprecipitation assay buffer (Sigma-Aldrich) complemented with EDTA-free protease inhibitor (Roche Diagnostics, Bromma, Sweden), sonicated for 5 min, and centrifuged at $20{,}000 \times g$ for 15 min. Protein concentration was measured using DC protein assay. PAD activity was measured using the Ab-Based Assay for PAD Activity (ModiQuest Research, Oss, the Netherlands) according to the manufacturer's instructions.

Immunohistochemical analysis

OC cultures were established on eight-well Falcon Chambered Cell Culture Slides (Fisher Scientific, Goteborg, Sweden), fixed with 2% formaldehyde (Sigma-Aldrich) at 4°C, and stored at −70°C until use. Endogenous peroxidase was blocked with 1% H_2O_2 for 1 h, followed by blocking of nonspecific Fc receptor binding using 20% AB human serum (Akademiska Pharmacy, Uppsala, Sweden) for 30 min. Slides were then incubated with rabbit polyclonal anti-PAD2 (Cosmobio, Tokyo, Japan) and anti-PAD4 (Abcam, Cambridge, U.K.) primary Abs, diluted in PBS containing 0.1% saponin for 90 min at room temperature at a final concentration of 0.02 μg/ml for the anti-PAD2 Ab and 1 μg/ml for the anti-PAD4 Ab. Cells were then washed and blocked with 1% normal goat serum (Dako, Stockholm, Sweden) for 15 min. Staining was developed using a secondary, HRP-conjugated goat anti-rabbit Ab (Vector Laboratories, Peterborough, U.K.) and visualized with 3,3-diaminobenzidene for 7 min. Slides were counterstained with Mayer's hematoxylin, dehydrated, and permanently mounted and viewed by light microscope (Reichert Polyvar 2 type 302001; Leica).

Immunofluorescence

Cells were washed twice with PBS followed by incubation with biotinylated 10-μg/ml 1325:04C03-ACPA (12), a 1:300 dilution of anti-human vimentin (PA527231; Life Technologies, Paisley, U.K.), or anti-human actin (A2066; Sigma-Aldrich) Abs in normal culture medium with 5 μg/ml Human BD Fc Block (BD Pharmingen) for 30 min on ice. Streptavidin–Alexa Fluor 594 conjugate, Alexa Fluor 488–conjugated goat anti-rabbit IgG (Thermo Fisher Scientific), and DAPI were incubated with cells in PBS for 45 min on ice to detect 1325:04C03-ACPA, vimentin, actin, and nuclei, respectively. Slides were washed by PBS and fixed in 2% paraformaldehyde for 15 min. A confocal Leica TCS SP5 microscope was used for acquiring the fluorescence microscopy images.

Statistical analysis

Multiple comparisons were performed using one-way ANOVA followed by Holm–Sidak post hoc test. GraphPad version 6.0 was used for the graphical analysis, and p values <0.05 were considered significant.

Results

iDCs can develop into mature OCs

To characterize the capacity of different cellular precursors to develop into OCs, PB $CD14^+$ monocytes were differentiated into either $CD14^-CD1a^+$ iDCs in the presence of GM-CSF and IL-4 or $CD14^+CD1a^-$ MΦs in the presence of M-CSF (Fig. 1A). Both cell types were further developed into OCs in the presence of RANKL and M-CSF. PCA of the protein expression data obtained with mass spectrometry revealed distant expression profiles in MΦs as compared with iDCs and in early-stage OCs developing from both precursor populations. On the contrary, almost identical protein expression profiles were detected in MΦ- and iDC-derived mature OCs (Fig. 1B). Detailed analysis of MΦ-, DC-, and OC-specific markers in the mass spectrometry data revealed that during iDC–OC transition, the DC marker CD1b was downregulated, while two of the MΦ markers, CD14 and CD68, were upregulated. OCs developing from both precursor populations were characterized by a comparable upregulation of cathepsin K and expressed similarly high levels of vimentin, demonstrating equally efficient OC maturation programs triggered in both iDCs and MΦs (Fig. 1C). Differentiation plasticity in developing iDCs has been shown to strongly depend on culture conditions, particularly cell concentrations (6, 13). In line with these studies, we observed distinct overall protein expression in iDCs obtained from dense and sparse cultures, indicating that these cells represent unique DC lineages (Fig. 2A), which was further supported by their capacity to develop into OCs. iDCs derived from dense cultures efficiently differentiated into OCs, whereas iDCs derived from sparse cultures had little or no capacity for OC development (Fig. 2B).

iDC–OC transdifferentiation is dependent on protein citrullination by PAD enzymes

To test whether citrullination can regulate iDC–OC transdifferentiation, we analyzed PAD expression and activity in different iDC types and during different stages of iDC–OC transition. Dense iDC cultures resulted in potent OC formation, and this was associated with higher PAD activity and levels of protein citrullination as compared with sparse DC cultures, which showed low capacity for OC formation (Fig. 2C, 2F). PAD activity in dense iDC cultures was comparable with the PAD activity in mature OCs (Fig. 2D). Citrullinated actin and vimentin were identified in the dense iDC cultures (Table I). In iDCs, we observed three citrullinated residues in actin, whereas in DC-derived OCs, eight citrullination sites were detected in actin and five in vimentin (Table I). Using immunohistochemistry, we observed an increasing expression and cytoplasmic location of PAD2 during OC differentiation, whereas

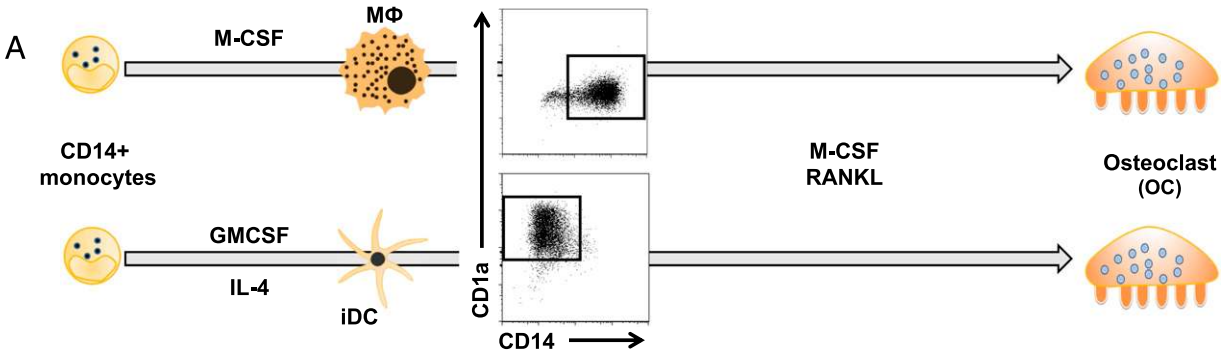

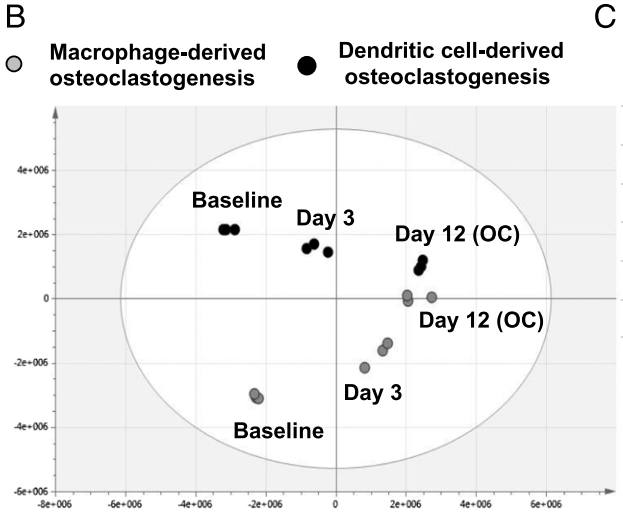

C

	DC	OC_{DC}	MΦ	$OC_{MΦ}$
CD1b	9.51 ± 0.16	6.75 ± 0.76	ND	ND
CD14	8.15± 0.40	10.55 ± 0.12	10.88 ± 0.005	10.69 ± 0.03
CD68	8.90 ± 0.06	9.46 ± 0.12	10.06 ± 0.07	9.70 ± 0.10
Cathepsin K	ND	8.34 ± 0.77	ND	9.38 ± 0.13
Vimentin	12.58 ± 0.004	12.70 ± 0.03	12.32 ± 0.01	12.68 ± 0.02

ND –represents not detectable

FIGURE 1. OC development from MΦ and DC precursors. (**A**) Schematic representation of OC development from MΦ and DCs. CD14 and CD1a expression was measured by flow cytomtery. (**B**) Protein abundances were determined in samples from three different stages of DC- and MΦ-derived OC development by mass spectrometry and label-free quantification and analyzed by PCA. Principal components 1 and 2 of triplicate samples from day 0 (iDC and MΦ), day 3 (intermediate stage), and day 12 (mature OCs) are plotted. (**C**) Expression of characteristic MΦ, DC, and OC markers were quantified using mass spectrometry, and the values in the table represent protein abundances that are $\log_{10}$-transformed. Mean ± SD values are calculated from triplicate samples.

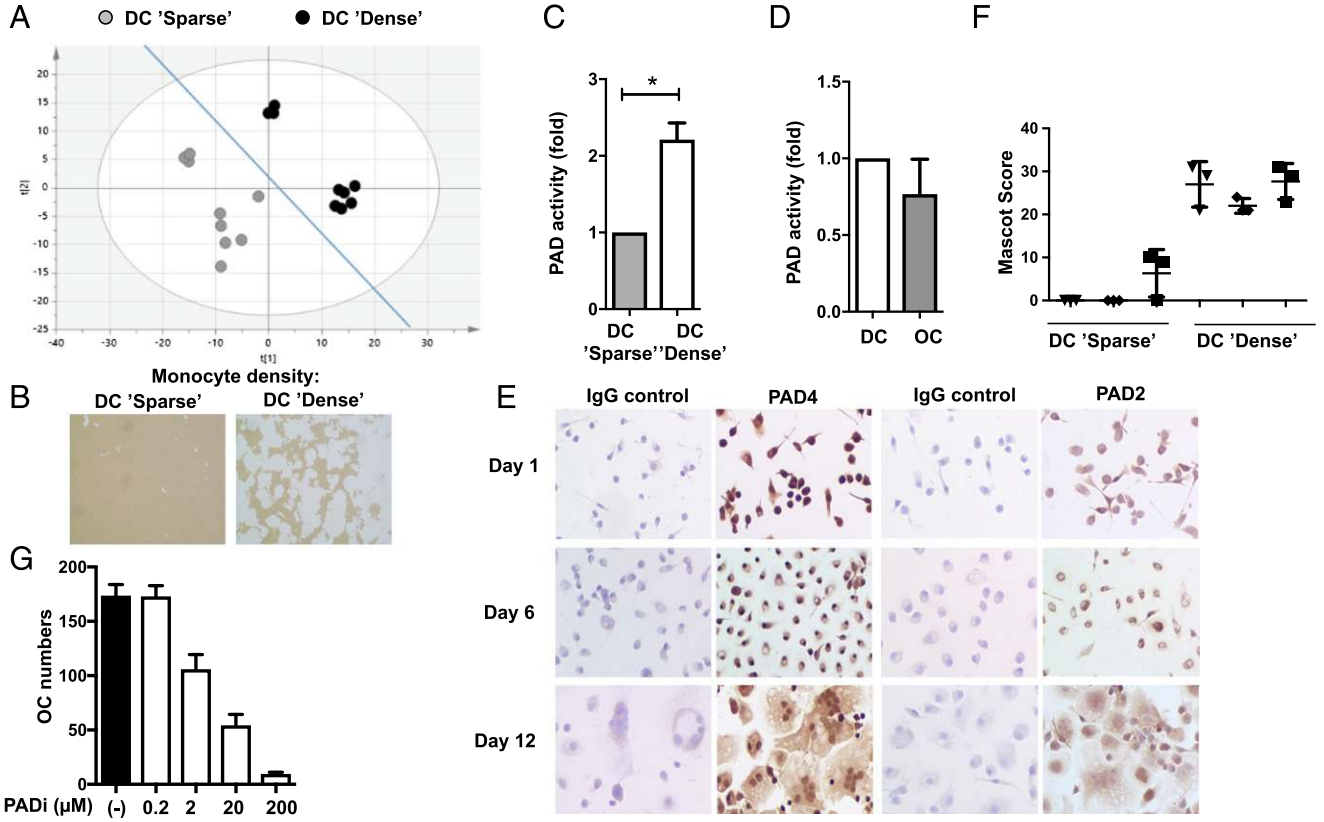

FIGURE 2. Protein citrullination and high PAD activity levels are associated with differentiation plasticity toward OCs in iDCs. (**A**) PCA indicates clearly distinct protein profiles in DCs obtained from sparse or dense cultures (principal components 1 and 2 are shown). Triplicate samples were analyzed from three independent experiments. (**B**) Images showing resorption activity on calcium phosphate–coated surface representing OCs that were generated from sparse or dense culture–derived iDCs (original magnification ×40). (**C**) Higher PAD activity was observed in the lysates of DCs that were obtained from dense cultures. Activity levels are normalized to sparse cultures; the graph represents four individual experiments, each with three replicates. *$p < 0.05$. (**D**) Normalized PAD activity levels are shown in cell lysates of iDCs and mature OCs. (**E**) Immunohistochemistry images indicate 3,3-diaminobenzidene staining of PAD4 and PAD2 enzymes with their respective irrelevant controls during OC development from DC precursors. Slides were counterstained with Mayer's hemotoxylin and analyzed in light microscopy (original magnification ×100). (**F**) Citrullinated actin was identified using mass spectrometry in lysates of DCs developing in sparse or dense cultures. The graph shows Mascot score values obtained for the identified peptide; symbols represent three different DC cultures. Mean ± SD values are shown. (**G**) Reduced DC–OC transdifferentiation in the presence of the PAD inhibitor Cl-amidine.

PAD4 expression was high and dominantly nuclear during all phases of iDC–OC transition, with a faint cytoplasmic staining in the mature OCs (Fig. 2E). PAD2 and PAD4 expression and a detectable protein citrullination during DC-derived OC development might indicate a role for protein citrullination in the transition of DCs into OCs, and in line with this hypothesis, we observed dose-dependent inhibition of iDC–OC transdifferentiation in the presence of Cl-amidine, a PAD inhibitor (Fig. 2G). Furthermore, protein citrullination was detected in dense iDC cultures but not in sparse cultures that did not promote OC development.

Citrullinated proteins are targeted by ACPAs on the surface of iDCs and iDC-derived OCs

Because vimentin and actin citrullination was detected in iDCs and/or iDC-derived OCs by mass spectrometry and a cell surface deposition of both of these proteins has been shown on other cell types (14, 15), we hypothesized that citrullinated actin and vimentin could be expressed on the surface of DC-derived OCs, providing potential target epitopes for ACPAs in RA patients. To test this hypothesis, we stained living, nonpermeabilized iDC-derived OCs with Abs against vimentin and actin as well as with an in-house engineered monoclonal ACPA, 1325:04C03 (12). Both actin and vimentin were expressed on the cell surface of iDC-derived OCs, showing a partial colocalization with cell-bound ACPAs (Fig. 3A, 3B).

We and others have previously reported that ACPAs can induce OC development from MΦs (7, 9), and therefore, we analyzed whether iDCs could also turn into OCs more efficiently in response to ACPAs. iDCs were generated using monocytes of healthy donors or ACPA-positive RA patients, and the cells were further developed into OCs in the presence or absence of ACPAs. ACPAs increased OC numbers and bone erosion from iDCs of both healthy donors (Fig. 4A) and ACPA-positive RA patients in comparison with IgG treatment (Fig. 4B). At a concentration of 1 μg/ml, ACPAs significantly increased the OC numbers (fold increase ± SD of 1.8 ± 0.57 in the case of healthy subjects and 2.22 ± 0.55 in the case of RA patients) and bone erosion (fold increase ± SD of 1.86 ± 0.50 in healthy subjects and 2.55 ± 0.11 in RA patients). ACPAs increased OC numbers in a dose-dependent fashion, with the effect reaching a plateau at a concentration of 5 μg/ml (Fig. 4C). Furthermore, $F(ab')_2$ fragments of the ACPAs, but not of the control Abs, were able to stimulate OC differentiation, suggesting that ACPA-mediated increase in OC is at least partially mediated by triggering key surface Ags by ACPAs (Fig. 4D). Importantly, ACPAs had a similar stimulatory effect when tested in OC cultures derived from circulating $CD1c^+$ myeloid DCs of healthy individuals, indicating that the observed mechanism is not restricted to the monocyte-derived DC model (Fig. 4E). Targeting PAD enzymes using Cl-amidine in the presence of ACPAs led to a decrease in ACPA-mediated OC increase, reiterating the importance of citrullination (Fig. 4F).

Table I. Identification of citrullinated targets in iDCs and OCs

Peptide Sequence	Amino Acid	DCs	Intermediate Stage	OCs
Actin				
AGFAGDDAP(Cit)AVFPSIVGRPR	19–39	28	—	26
AVFPSIVG(Cit)PR	29–39	—	—	10
(Cit)GILTLK	62–68	—	3	46
IWHHTFYNEL(Cit)VAPEEHPVLLTEAPLNPK	85–113	41	—	46
ILTE(Cit)GYSFTTTAER	192–206	—	—	41
GYSFTTTAE(Cit)EIVR	197–210	—	—	44
DLYANTVLSGGTTMYPGIAD(Cit)MQK	292–315	—	—	11
QEYDESGPSIVH(Cit)K	360–373	31	20	37
Vimentin				
SLYASSPGGVYAT(Cit)SSAVR	51–69	—	—	68
NT(Cit)TNEKVELQELNDR	98–113	—	—	124
DV(Cit)QQYESVAAK	271–282	—	—	44
FADLSEAAN(Cit)NNDALR	295–310	—	—	42
KLLEGEES(Cit)SLPLPNFSSLNLR	402–424	—	—	42
LLEGEES(Cit)SLPLPNFSSLNLR	403–424	—	—	39

Numbers indicate the highest Mascot score for each identified citrullinated peptide from three independent replicates. An en dash (—) indicates that the citrullinated peptide was not detected.

IL-8 regulates ACPA-induced DC–OC transdifferentiation

Various cytokines can influence the development of OCs, including TNF, IL-6, and IL-8, which promote differentiation, or IL-10, which possesses an inhibitory effect. To investigate the effect of cytokines in the ACPA-mediated regulation of DC-derived osteoclastogenesis, we screened for the presence of a set of cytokines and chemokines in the supernatants at three time points during the DC–OC transdifferentiation. We detected significantly elevated IL-8 levels in the supernatants of ACPA-treated OC cultures as compared with untreated or control IgG-treated samples (Fig. 5A), whereas IL-6 levels remained unaffected by the presence of ACPAs, and TNF and IL-10 were not detectable (Fig. 5B). In addition, F(ab')$_2$ fragments of the ACPAs, but not of the control Abs, were able to stimulate IL-8 secretion in the OC cultures (Fig. 5C). The receptors for IL-8, CXCR1, and CXCR2 were both present on the surface of the majority of iDCs (Fig. 5D). IL-8 neutralizing Abs completely abolished the ACPA-induced osteoclastogenesis (Fig. 5E), demonstrating a crucial role for IL-8 in diverting DCs toward bone-erosive functions in the presence of ACPAs.

Discussion

Increased osteoclastogenesis is an early pathogenic feature of inflammatory arthritis, and specifically of ACPA-positive RA. In

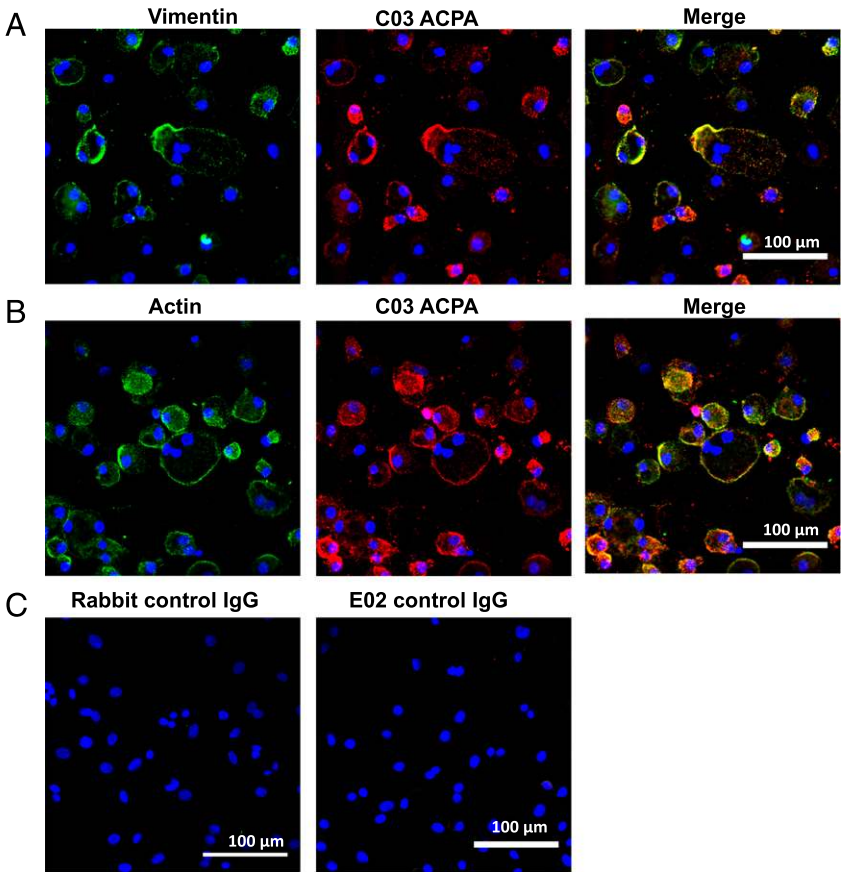

FIGURE 3. Citrullinated actin and vimentin are potential ACPA targets on the surface of iDC-derived OCs. Confocal microscopy images displaying vimentin (**A**) or actin (**B**) localization in green and ACPA (clone 1325:04C03) binding in red on the surface of iDCs or DC-derived OCs (original magnification ×400). (**C**) Staining with the control IgG for ACPA and vimentin or actin. Nuclear stainings using DAPI are indicated in blue. In the last panels, the images respresent the ACPA staining merge with actin or vimentin; yellow coloring indicates colocalization of the tested proteins with monoclonal ACPA.

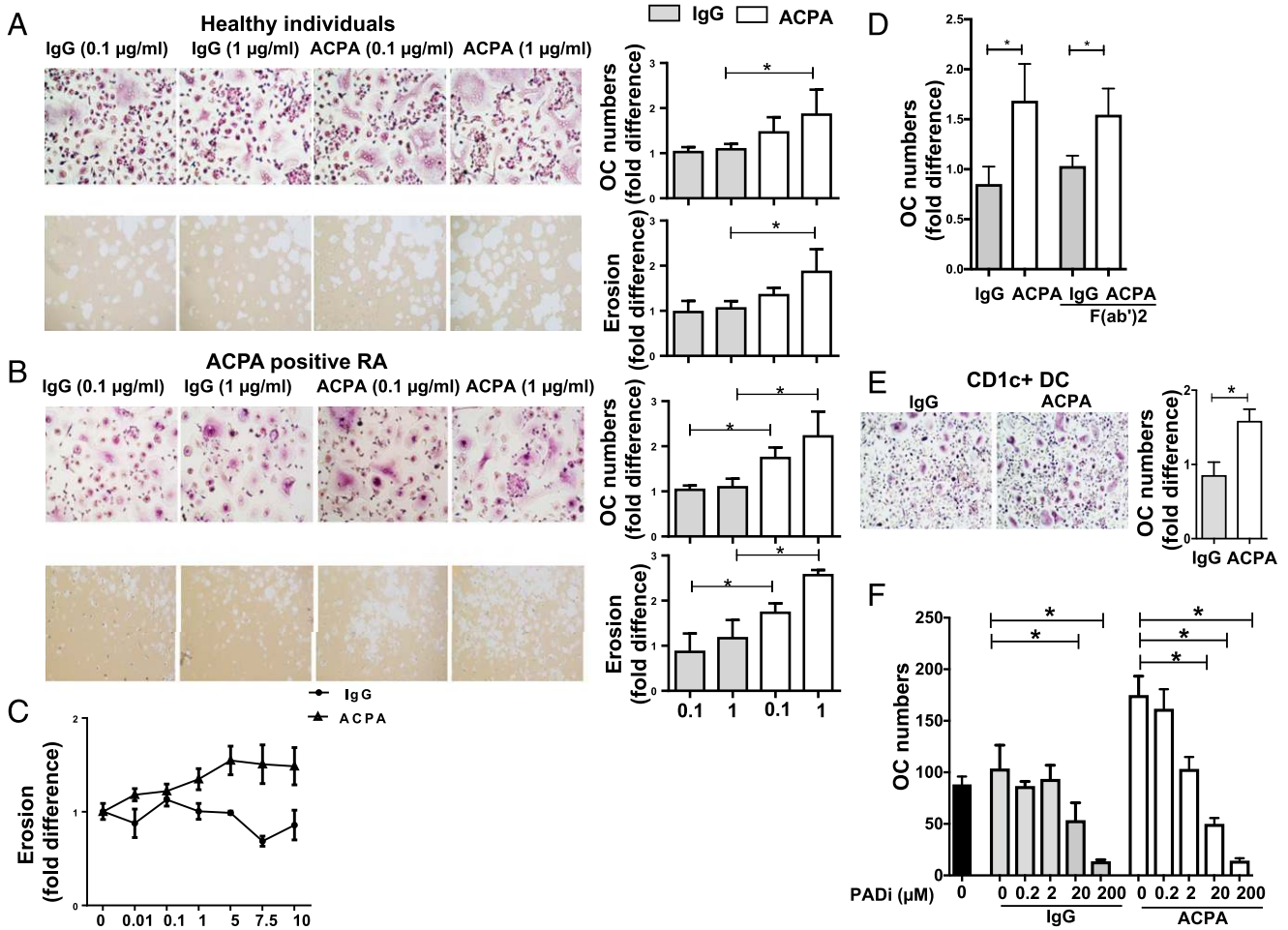

FIGURE 4. Targeting citrullinated cell surface proteins by ACPAs induces DC–OC transdifferentiation. TRAP staining (upper panels) and bone resorption assays (lower panels) representing OC cultures generated from monocyte-derived iDCs derived from the PB of healthy individuals (**A**) and RA patients (**B**). The iDCs were cultured in the presence of 0.1 or 1 μg/ml ACPAs or control IgG. The images were obtained using light microscopy [(A and B) original magnification ×200 (top row), ×40 (bottom row)]. The graphs represent the fold difference (normalized using controls M-CSF/RANKL but no Abs) in OC numbers and in resorption areas. Mean ± SD values were calculated from at least three independent experiments. (**C**) ACPAs or control IgGs were applied at different concentrations during DC-derived OC development; OC activity was measured in bone erosion assay (normalized to controls receiving M-CSF/RANKL but no Abs). (**D**) $F(ab')_2$ ACPAs induced an increase in OC development. The graph represents the OC numbers developing in the presence of $F(ab')_2$ ACPA and ACPA Ab with their respective control IgGs. Mean ± SD values were calculated from at least three independent experiments. (**E**) $CD1c^+$ DCs were isolated from PB of healthy individuals, and the cells were cultured in the presence of M-CSF, RANKL, and ACPAs or control IgG. OCs were visualized using TRAP staining (original magnification ×100); the graph represents normalized values obtained from three independent experiments. (**F**) The PAD inhibitor Cl-amidine prevented the ACPA-induced increase in OC development. Cl-amidine was used in concentrations of 0.2, 2, 20, and 200 μM, and IgG and ACPA concentrations were 1 μg/ml. The graph represents OC numbers developing in the presence of IgG or ACPA. Mean ± SD values were calculated in triplicate wells; representative results from three independent experiments are shown. $*p < 0.05$.

this work, we have demonstrated that DCs can be converted to potent OC precursors through an increase in protein citrullination and the binding of ACPAs to the cell surface, which promoted IL-8 release by the cells. The transdifferentiation of DCs into OCs might represent an important, novel mechanism that contributes to bone destruction in ACPA-positive RA and could be sensitively regulated by blocking either citrullination or IL-8 binding to its receptor molecules.

We observed that iDCs were characterized by a strikingly different protein profile as compared with MΦs but nevertheless showed a remarkably similar capacity to develop into OCs when exposed to M-CSF and RANKL. The ability of iDCs to transdifferentiate into OCs has been previously shown in murine experimental models (16, 17) in vitro and also in vivo when DCs were injected into OC-deficient animals (17). We and others have also shown that iDCs generated from the PB monocytes of healthy volunteers are able to transdifferentiate into OCs (6, 7, 18). In this study, we extended these findings by demonstrating that both iDCs derived from monocytes of RA patients and circulating $CD1c^+$ iDCs of healthy individuals could transdifferentiate into OCs. To our knowledge, this is a previously unrecognized feature of the $CD1c^+$ iDCs that dominates the PB myeloid DC compartment and is enriched in the inflamed RA synovium (19, 20).

Apart from the need for RANKL and the M-CSF requirement, little is known about the mechanisms governing iDC–OC transdifferentiation. On the one hand, DC–OC transdifferentiation might simply be a consequence of chronic exposure to proosteoclastogenic cytokines in the absence of other classical signals needed for DC-induced immune responses to occur. On the other hand, previous data suggest that the development of iDC-derived OCs might be a more complex event, with the commitment of DCs to Ag presentation or to alternative functions already being set during early phases of their differentiation (6, 21). In this context, a remarkable heterogeneity has been observed between DC subsets in their plasticity

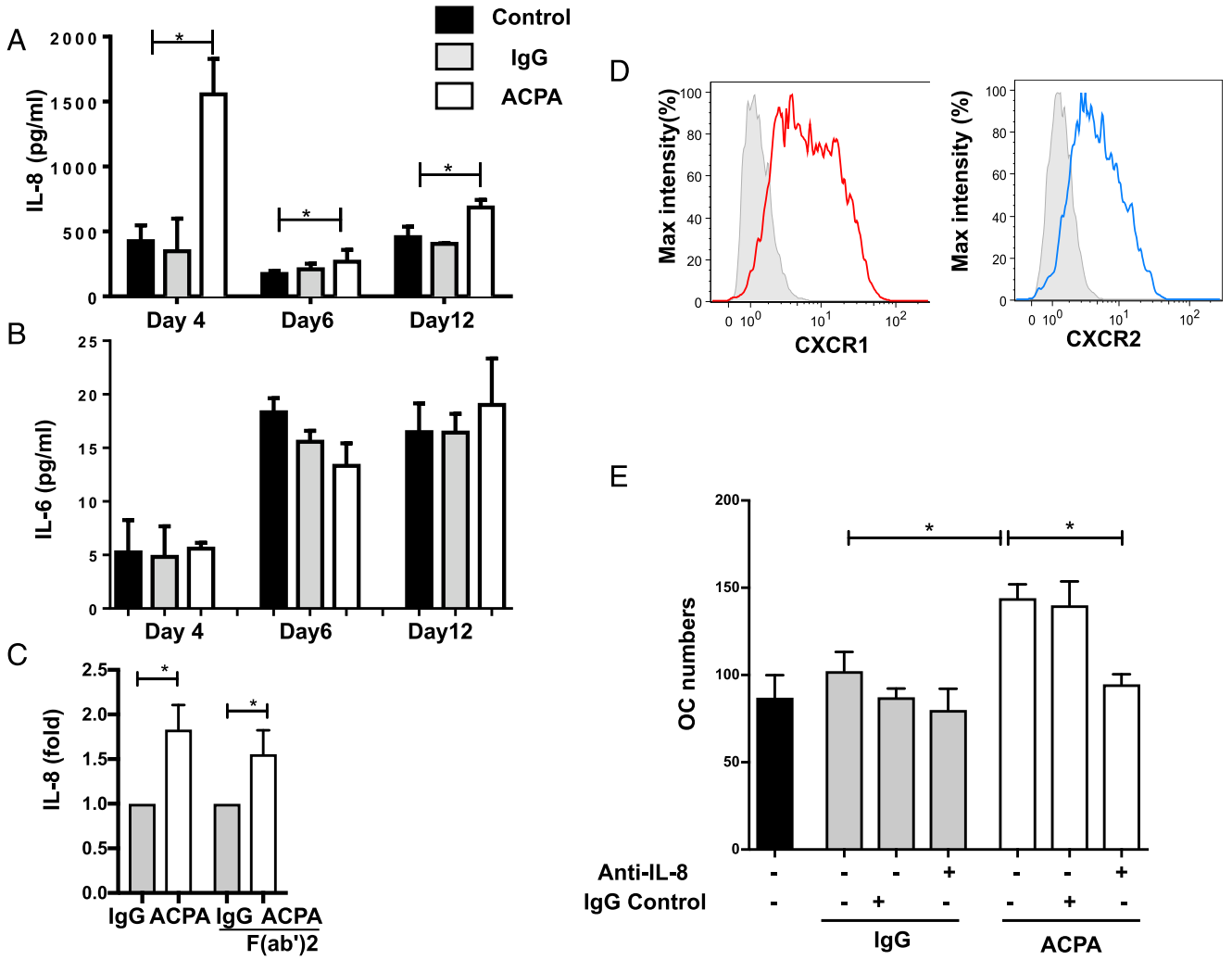

FIGURE 5. ACPAs regulate osteoclastogenesis through induction of IL-8. IL-8 (**A**) and IL-6 (**B**) levels were measured in the supernatants of DC-derived OC cultures at different time points using cytometric bead array. ACPAs and control IgG were added to culture at a final concentration of 1 μg/ml. Mean ± SD values were calculated from triplicate samples; representative data from three independent experiments are shown. (**C**) $F(ab')_2$ ACPAs induced increased IL-8 release. The graph shows the increase in the IL-8 levels mediated by $F(ab')_2$ ACPAs and ACPA Ab but not $F(ab')_2$ IgG or control IgG. (**D**) Expression of the IL-8Rs CXCR1 and CXCR2 was analyzed on iDCs using flow cytometry. Histograms in gray show stainings with isotype control Abs. (**E**) IL-8 neutralizing Abs abolished the stimulatory effects of ACPAs on OC differentiation. The graphs show OC numbers; mean ± SD values were calculated from triplicate samples. *$p < 0.05$.

toward OC differentiation. Splenic $CD4^-CD8^-$ DCs are potent OC precursors, whereas the $CD4^+CD8^-$ and the $CD8^+$ murine DC subsets have little or no capacity for OC transdifferentiation but instead can efficiently activate cytotoxic T cell responses (17). Furthermore, we have previously reported a marked heterogeneity among human monocyte-derived iDCs in their capacity for developing into OCs. Higher cell concentrations applied at early stages of DC development increased differentiation plasticity toward OCs at least partly through the accumulation of lactic acid in the cultures (6). On the contrary, DCs developing in sparse cultures resulted in a high level of immunogenicity with very little OC transdifferentiation potential. Interestingly, we show in this study that the dense OC-prone iDC cultures are characterized by higher PAD activity than the sparse iDC cultures. This is accompanied by detectable levels of citrullinated peptides, specifically citrullinated actin and vimentin, in the dense iDC cultures, in contrast to the less osteoclastogenic sparse iDC cultures or MΦs. Confocal microscopy evaluation of the living cell stainings confirmed ACPA binding and the presence of vimentin and actin on the surface of the OCs. Partial colocalization should be interpreted in the context of a low amount of citrullination affecting a given protein (22), with ACPA binding occurring on the citrullinated version only, whereas actin and vimentin are stained irrespectively of citrullination. Notably, citrullination may not exclusively occur in actin and vimentin but possibly also in other proteins that may not be abundant enough to allow detection using mass spectrometry. These data suggest a potential role for citrullination in the iDC–OC transdifferentiation, a hypothesis that is further supported by the profound inhibition of OC development in the presence of the PAD inhibitor Cl-amidine, independent of IL-8 production (data not shown). Furthermore, in accordance with our previous findings on MΦ-derived OC differentiation (7), we show in this study that Abs against citrullinated proteins could bind to human iDCs in vitro and enhance OC development in an Fc-independent, IL-8–dependent autocrine manner. The partial colocalization of the monoclonal ACPA with both vimentin and actin on the cell surface of DC-derived OCs strongly suggests that citrullination of these proteins and their relocation to the plasma membrane facilitate the effects of ACPAs on these cells. Although it is not known whether citrullinated actin and vimentin could be

selectively enriched on the cell surface, it has been previously shown that PAD enzymes are recruited to autophagic vesicles where citrullinated peptides are generated for MHC class II–dependent Ag presentation in DCs (23). It is intriguing to speculate that protein citrullination in an autophagic compartment may not only generate peptides for MHC presentation but could concomitantly facilitate a constant flow of citrullinated proteins to the cell surface. In summary, citrullination appears to be required not only for the steady-state iDC–OC transdifferentiation in the presence of osteoclastogenic factors but also for the ACPA-enhanced iDC–OC transdifferentiation in individuals in whom these autoantibodies are generated.

In conclusion, our results identify iDCs as important precursors for OC development in both healthy and diseased conditions. We showed that the plasticity of iDC transdifferentation into OCs is dependent on protein citrullination, and it is enhanced by the RA-specific ACPAs through an IL-8–dependent mechanism. Selective modulation of either PAD enzymes or ACPA-induced chemokine production might, thus, represent an important strategy to limit OC development and promote bone regeneration in ACPA-positive individuals.

Acknowledgments

The authors acknowledge the excellent technical assistance from Lena Israelsson and Marianne Engström.

Disclosures

The authors have no financial conflicts of interest.

References

1. Steinman, R. M., and J. Banchereau. 2007. Taking dendritic cells into medicine. *Nature* 449: 419–426.
2. Steinman, R. M., D. Hawiger, and M. C. Nussenzweig. 2003. Tolerogenic dendritic cells. *Annu. Rev. Immunol.* 21: 685–711.
3. Thomson, A. W., and P. D. Robbins. 2008. Tolerogenic dendritic cells for autoimmune disease and transplantation. *Ann. Rheum. Dis.* 67(Suppl. 3): iii90–iii96.
4. O'Neill, L. A., R. J. Kishton, and J. Rathmell. 2016. A guide to immunometabolism for immunologists. *Nat. Rev. Immunol.* 16: 553–565.
5. Rivollier, A., M. Mazzorana, J. Tebib, M. Piperno, T. Aitsiselmi, C. Rabourdin-Combe, P. Jurdic, and C. Servet-Delprat. 2004. Immature dendritic cell transdifferentiation into osteoclasts: a novel pathway sustained by the rheumatoid arthritis microenvironment. *Blood* 104: 4029–4037.
6. Nasi, A., T. Fekete, A. Krishnamurthy, S. Snowden, E. Rajnavölgyi, A. I. Catrina, C. E. Wheelock, N. Vivar, and B. Rethi. 2013. Dendritic cell reprogramming by endogenously produced lactic acid. *J. Immunol.* 191: 3090–3099.
7. Krishnamurthy, A., V. Joshua, A. Haj Hensvold, T. Jin, M. Sun, N. Vivar, A. J. Ytterberg, M. Engström, C. Fernandes-Cerqueira, K. Amara, et al. 2016. Identification of a novel chemokine-dependent molecular mechanism underlying rheumatoid arthritis-associated autoantibody-mediated bone loss. [Published erratum appears in 2019 *Ann. Rheum. Dis.*] *Ann. Rheum. Dis.* 75: 721–729.
8. Kleyer, A., S. Finzel, J. Rech, B. Manger, M. Krieter, F. Faustini, E. Araujo, A. J. Hueber, U. Harre, and K. Engelke. 2014. Bone loss before the clinical onset of rheumatoid arthritis in subjects with anticitrullinated protein antibodies. *Ann. Rheum. Dis.* 73: 854–860.
9. Harre, U., D. Georgess, H. Bang, A. Bozec, R. Axmann, E. Ossipova, P.-J. Jakobsson, W. Baum, F. Nimmerjahn, E. Szarka, et al. 2012. Induction of osteoclastogenesis and bone loss by human autoantibodies against citrullinated vimentin. *J. Clin. Invest.* 122: 1791–1802.
10. Ossipova, E., C. F. Cerqueira, E. Reed, N. Kharlamova, L. Israelsson, R. Holmdahl, K. S. Nandakumar, M. Engström, U. Harre, G. Schett, et al. 2014. Affinity purified anti-citrullinated protein/peptide antibodies target antigens expressed in the rheumatoid joint. *Arthritis Res. Ther.* 16: R167.
11. Lyutvinskiy, Y., H. Yang, D. Rutishauser, and R. A. Zubarev. 2013. In silico instrumental response correction improves precision of label-free proteomics and accuracy of proteomics-based predictive models. *Mol. Cell. Proteomics* 12: 2324–2331.
12. Steen, J., B. Forsström, P. Sahlström, V. Odowd, L. Israelsson, A. Krishnamurthy, S. Badreh, L. Mathsson Alm, J. Compson, and D. Ramsköld. 2019. Recognition of amino acid motifs, rather than specific proteins, by human plasma cell-derived monoclonal antibodies to posttranslationally modified proteins in rheumatoid arthritis. *Arthritis Rheumatol.* 71: 196–209.
13. Nasi, A., V. P. Bollampalli, M. Sun, Y. Chen, S. Amu, S. Nylén, L. Eidsmo, A. G. Rothfuchs, and B. Réthi. 2017. Immunogenicity is preferentially induced in sparse dendritic cell cultures. *Sci. Rep.* 7: 43989.
14. Shigyo, M., T. Kuboyama, Y. Sawai, M. Tada-Umezaki, and C. Tohda. 2015. Extracellular vimentin interacts with insulin-like growth factor 1 receptor to promote axonal growth. *Sci. Rep.* 5: 12055.
15. Sozzani, S., M. Rusnati, E. Riboldi, S. Mitola, and M. Presta. 2007. Dendritic cell-endothelial cell cross-talk in angiogenesis. *Trends Immunol.* 28: 385–392.
16. Speziani, C., A. Rivollier, A. Gallois, F. Coury, M. Mazzorana, O. Azocar, M. Flacher, C. Bella, J. Tebib, P. Jurdic, et al. 2007. Murine dendritic cell transdifferentiation into osteoclasts is differentially regulated by innate and adaptive cytokines. *Eur. J. Immunol.* 37: 747–757.
17. Wakkach, A., A. Mansour, R. Dacquin, E. Coste, P. Jurdic, G. F. Carle, and C. Blin-Wakkach. 2008. Bone marrow microenvironment controls the in vivo differentiation of murine dendritic cells into osteoclasts. *Blood* 112: 5074–5083.
18. Tucci, M., S. Ciavarella, S. Strippoli, O. Brunetti, F. Dammacco, and F. Silvestris. 2011. Immature dendritic cells from patients with multiple myeloma are prone to osteoclast differentiation in vitro. *Exp. Hematol.* 39: 773–783.e1.
19. Moret, F. M., C. E. Hack, K. M. van der Wurff-Jacobs, W. de Jager, T. R. Radstake, F. P. Lafeber, and J. A. van Roon. 2013. Intra-articular CD1c-expressing myeloid dendritic cells from rheumatoid arthritis patients express a unique set of T cell-attracting chemokines and spontaneously induce Th1, Th17 and Th2 cell activity. *Arthritis Res. Ther.* 15: R155.
20. Jongbloed, S. L., M. C. Lebre, A. R. Fraser, J. A. Gracie, R. D. Sturrock, P. P. Tak, and I. B. McInnes. 2006. Enumeration and phenotypical analysis of distinct dendritic cell subsets in psoriatic arthritis and rheumatoid arthritis. *Arthritis Res. Ther.* 8: R15.
21. Gallois, A., J. Lachuer, G. Yvert, A. Wierinckx, F. Brunet, C. Rabourdin-Combe, C. Delprat, P. Jurdic, and M. Mazzorana. 2010. Genome-wide expression analyses establish dendritic cells as a new osteoclast precursor able to generate bone-resorbing cells more efficiently than monocytes. *J. Bone Miner. Res.* 25: 661–672.
22. Ytterberg, A. J., V. Joshua, G. Reynisdottir, N. K. Tarasova, D. Rutishauser, E. Ossipova, A. H. Hensvold, A. Eklund, C. M. Sköld, and J. Grunewald. 2015. Shared immunological targets in the lungs and joints of patients with rheumatoid arthritis: identification and validation. *Ann. Rheum. Dis.* 74: 1772–1777.
23. Ireland, J. M., and E. R. Unanue. 2011. Autophagy in antigen-presenting cells results in presentation of citrullinated peptides to CD4 T cells. *J. Exp. Med.* 208: 2625–2632.